ARMA 22–413

Comparative Analysis of Synthetic and Steel Mesh Performance

Benton, D.J., Sweet, D.J., Emery, T.M.
National Institute for Occupational Safety and Health, Spokane, Washington, USA

This paper was prepared for presentation at the 56th US Rock Mechanics/Geomechanics Symposium held in Santa Fe, New Mexico, USA, 26-29 June 2022. This paper was selected for presentation at the symposium by an ARMA Technical Program Committee based on a technical and critical review of the paper by a minimum of two technical reviewers. The material, as presented, does not necessarily reflect any position of ARMA, its officers, or members. Electronic reproduction, distribution, or storage of any part of this paper for commercial purposes without the written consent of ARMA is prohibited. Permission to reproduce in print is restricted to an abstract of not more than 200 words; illustrations may not be copied. The abstract must contain conspicuous acknowledgement of where and by whom the paper was presented.

ABSTRACT: The Spokane Mining Research Division (SMRD), of the U.S. National Institute for Occupational Safety and Health (NIOSH) is continuing research on the mechanical behavior of primary surface support components in mining ground support systems. Mining ground control safety often depends on supporting, or at least containing, the ground between rockbolts using what is referred to as local, surface, or areal ground support. Steel mesh, in various combinations and with other components, is often used to accomplish this, as well as to retain loose rock. Local ground support is an integral part of maintaining a safe underground operation. However, as underground hard rock mining continues moving towards automation, increased challenges regarding support installation and maintenance will create a need for a new generation of mesh support systems. Advanced materials engineering has created various synthetic meshes to meet this need. This study begins a process of compiling technical information on multiple types of mesh performance, leading to an eventual comprehensive index for industry use. Using SMRD's high-energy high-deformation (HEHD) testing machine, a program was developed to assess the behavior of a variety of steel and synthetic mesh products in quasi-static loading conditions. The data from these tests were used for comparative analyses of the force-displacement and energy-displacement characteristics of conventional steel meshes to synthetic meshes. Considerations were also given to several additional operational and performance factors, including corrosivity, flammability, durability, and handling. This work was completed as part of the SMRD mission of improving the health and safety of underground metal mine workers, and this paper presents the findings of these tests.

1. INTRODUCTION

Mining in ground that may fail from the combination of in situ and mining induced stress is commonplace. Ground support elements are installed to reinforce such ground and preserve personnel and mine safety. Typically, the strength of support is considered key, and is used to prevent or halt ground failure. In stiff rock masses, confining stresses generated by the ground support system are very small compared with the stresses associated with rock fracture, and the support pressure will have no direct effect on fracture initiation (Ortlepp, 1969). However, ground movements driven by creep of weak ground or seismic loading may be somewhat effectively managed by support that is able to yield with the ground in a safe manner while maintaining confining pressure on the rock in the immediate perimeter of the opening. In addition, it is usually desirable to contain ground between rockbolts to protect miners from loose rock that might fall or be ejected (Potvin and Hadjigeorgiou, 2020).

Rockburst damage in the form of rock bulking due to fracturing results in rapid expansion of rock volume (Kaiser, Tannant and McCreath, 1996). This causes sudden loading of the ground support system, which must be able to yield and absorb energy at high displacement rates. In the case of rock ejection, up to 1 m3 (35.3 ft3) of rock may be ejected at velocities as high as 6 m/s (20 fps) or more (Ortlepp and Stacey, 1998; Stacey, Ortlepp and Kirsten, 1995). Such loading will overcome the initial strength of most ground support systems; therefore the support must maintain its strength over large, rapid displacements to absorb the kinetic energy of the ejecting rock and bring it to rest (Wagner, 1984; Roberts and Brummer, 1988). The capacity for the ground support system to maintain strength over large deformations, or the ability to absorb energy – calculated for a given ground support system or component as the area under the force-displacement plot – is key to support effectiveness in squeezing and rockburst-prone ground (Potvin and Hadjigeorgiou, 2020; Kalenchuk, Palleske, Hume and Oke, 2020).

A complete ground support system is composed of three main components (Ortlepp, 1983; Potvin, Wesseloo and Heal, 2010): (1) reinforcement, such as bolts and cables, (2) containment, such as shotcrete and mesh, and (3) connections, such as plates, anchors, and grouting. Although reinforcement is the critical component that stabilizes the rock mass, any ground support system is only as effective as its weakest link (Potvin, Wesseloo and Heal, 2010). The containment component was selected as the focus for this study. Containment helps maintain stability of the rock mass between the bolts. Specifically, mesh, used as a standalone surface support, typically serves to prevent loose rock from falling into the excavation. Although mesh has high rupture strength and high deformability, it is not stiff until after significant displacement, on the order of 10 cm (4 in) or more (Pakalnis and Ames, 1983; Morton, Thompson and Villaescusa, 2007; Player, Morton and Villaescusa, 2008).

As Hadjigeorgiou and Stacey (2018) point out, despite surface support being an essential component of ground control systems, there exists no comprehensive reference index of the performance characteristics of multiple types of mesh. Researchers at the Spokane Mining Research Division (SMRD), of the U.S. National Institute for Occupational Safety and Health (NIOSH), responded to this deficiency by designing and testing on a full-scale test device to specifically account for large support system deformation (Martin et al., 2015, Raffaldi et al;, 2016, Raffaldi et al., 2018). A testing program assessing the behaviour of a variety of mesh products, including both steel (chain-link and welded wire) and synthetic options, experiencing large deformation has thus been initiated. This work is being completed as part of the SMRD mission of improving the health and safety of the nation's underground metal mine workers, and this paper presents the findings of these tests.

2. METHODOLOGY

The SMRD-developed test device used in this study, called the High-Energy and High-Deformation (HEHD) load frame, can be seen in Figure 1. This design improves upon the earlier work and is being used to advance industry understanding of the mechanical behavior of support meshes when used as surface support in a complete ground support system. The HEHD test frame specifications for the current test program were developed by modifying Kirsten and Labrum's (1990) test design. The new test frame includes a ram stroke of 60.0 cm (23.6 in), roughly quadrupling the test stroke of Kirsten and Labrum's design. Additionally, the test sample edge length was increased by 20 cm (7.9 in) from Kirsten and Labrum's design to accommodate a 1.2-m (4 ft) bolt patterns. A hemispherical loading ram was used to avoid an unrealistic punching type failure that often occurs if a point loading is applied to test specimens. Although Kirsten and Labrum (1990) and Tannant and Kaiser (1997) found that the geometry of the loading head — square plate versus pressurized bag — had minimal effect on test results, the spherical loading head avoids edge effects inherent in a square loading plate and is more durable than a pressurized bag. This type of loading is more representative of the rock bagging between the bolts that occurs in underground metal mines. The current test setup is shown in Figure 2. The mesh sample is stretched by hand over four rockbolts embedded in concrete reaction columns fixed to the reaction floor.

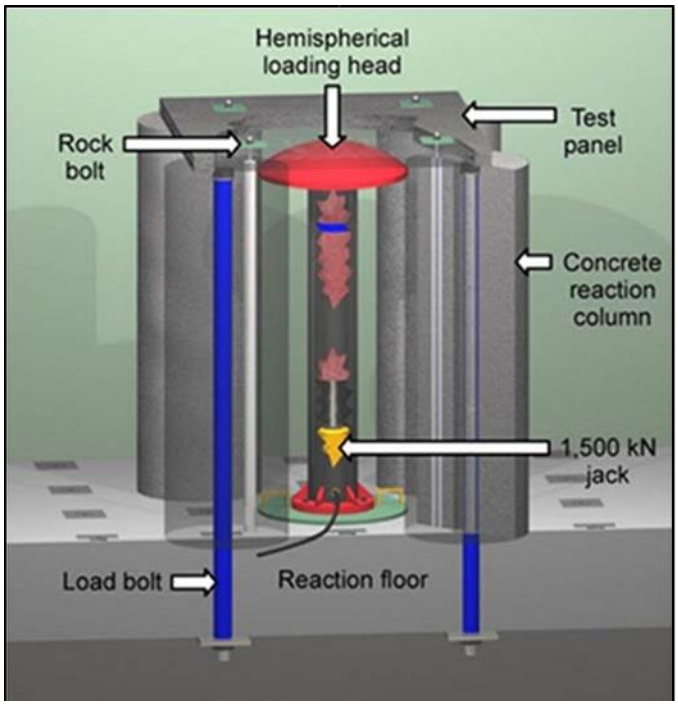

Fig. 1. Technical schematic of the high-energy high-deformation (HEHD) panel test machine.

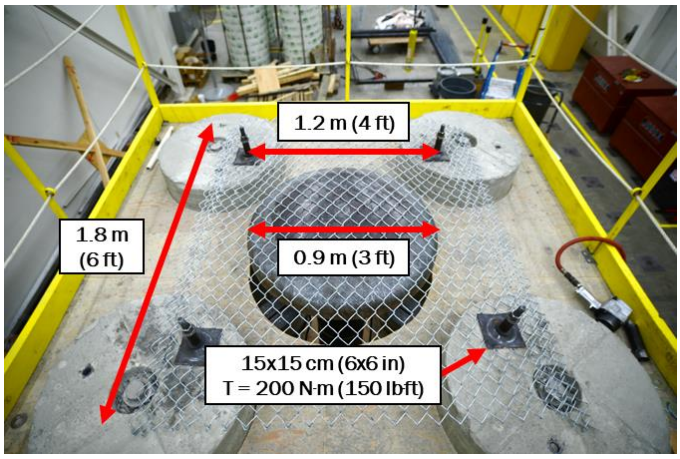

Fig. 2. HEHD mesh testing setup and dimensions using chain-link fencing.

For this study, the quasi-static loading response of three types of steel meshes (chain-link and two variations of welded wire) and two synthetic meshes were compared. The testing results of the chain-link and welded wire

meshes were used as an industry-standard baseline to which synthetic mesh options could be compared. This decision was made based on a general assumption that steel meshes are most commonly used in underground mines where areal surface support is needed. Factors including peak load and energy absorption capacity, along with loose rock containment capability, further led to the decision to establish the chain-link test results as the chief reference (i.e., all performance indicators equal 100%). The performance of the alternative synthetic meshes discussed in the remainder of this paper thus has a qualitative reference that can be more widely understood by industry.

3. DATA

Chain-link fencing, sometimes referred to as woven-wire, is a common type of steel mesh used for surface support of openings underground. Its flexibility allows for easy storage, transport, placement, and successful performance over large displacements. HEHD testing used 1.8x1.8-m (6x6-ft) samples of 5-cm (2-in) aperture 9 gauge chain-link fencing. The mesh was constrained only by the four reaction column rockbolts and 15-cm (6-in) square faceplates torqued to 200 N·m (150 ft·lbs). A post-test photo is shown in Figure 3, where the extensive deformation caused by the HEHD machine can be seen.

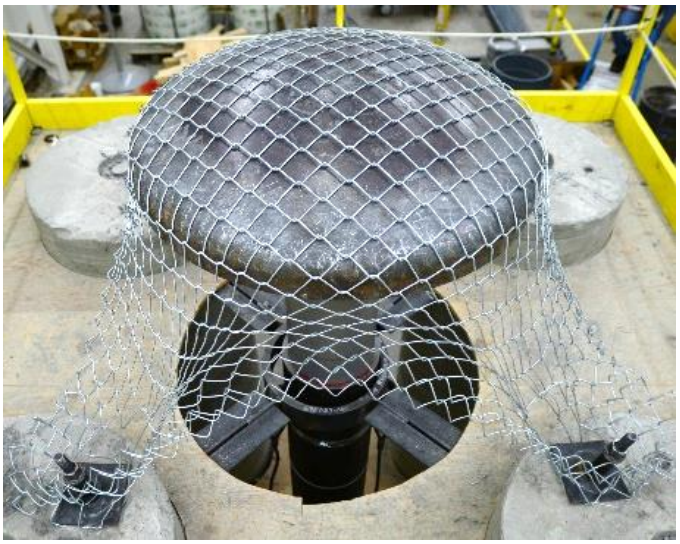

Fig. 3. Post-test photo of a chain-link test sample, maximum sample displacement.

To analyze the test results, the graph in Figure 4 shows the averages for the measured force-displacement and calculated energy-displacement graphs from the chain-link tests performed. The test results were highly reproducible, with a maximum load of 70 kN (15.7 kips) at 450 mm (17.7 in) of ram displacement, and a calculated cumulative energy absorption approaching 12.3 kJ (9072 ft·lbf) at 500 mm (20 in) displacement. Importantly, the mesh sample itself remained intact and pinned at all four bolts, indicating an ability to prevent significant rock falls at extraordinarily high displacements.

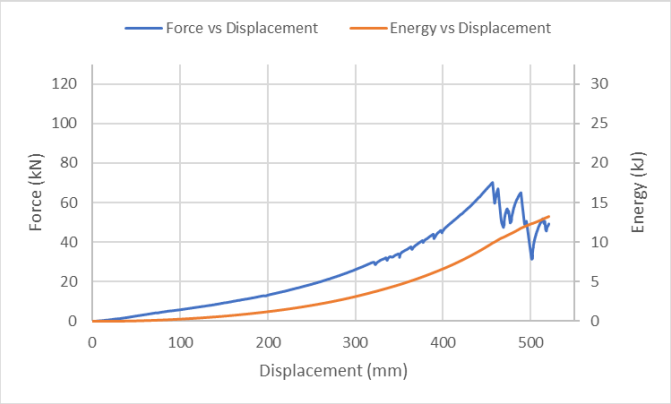

Fig. 4. Chain-link mesh representative testing results, force and energy versus displacement.

For comparison to chain-link mesh, 6-gauge 7.6-cm (3-in), and 10.1-cm (4-in) aperture welded wire mesh samples were tested. These are also relatively common in underground mining, typically installed as panels along the excavation walls. Sample size and affixation to the HEHD test frame were identical to those for the chain-link samples. Figure 5 shows the post-test status of one of the 10-cm (4-in) welded wire samples.

Fig. 5. Post-test photo welded wire test sample, maximum sample displacement.

The representative force-displacement and calculated energy-displacement curves for the 7.6-cm (3-in), and 10.1-cm (4-in) welded wire mesh tests are shown in Figures 6 and 7, respectively. The 10.1-cm (4-in) samples were the lower performing of the two, with maximum load reached at a ram displacement of only 300 mm (11.8 in), significantly less than the chain-link sample. The maximum load value itself of 37 kN (8.3 kips), and the energy-displacement value at 500 mm (19.7 in) of 8.4 kJ (6196 ft·lbf), were also significantly less than that of the chain-link values. The 7.6-cm (3-in) welded wire samples performed slightly better, with peak load and 500-mm (19.7-in) energy values of 53 kN (11.9 kips) and 11.4 kJ (8408 ft·lbf), respectively.

It is important to note, however, the observed tendency of the welded wire meshes to separate from the rockbolts pinning them to the reaction columns. The particular sample shown in Figure 5 separated from both front rockbolts. The first separation (front-right bolt) occurred at a ram energy-displacement point of 4.4 kJ (3245 ft·lbf) and 345 mm (13.6 in), and the second occurred at 5.8 kJ (4278 ft·lbf) and 420 mm (16.5 in). The effect of these separations was not only reduced energy absorption capacity, but also a reduced capability of rock fragment restriction at high displacements, especially when considered along with the already increased mesh aperture relative to chain-link mesh.

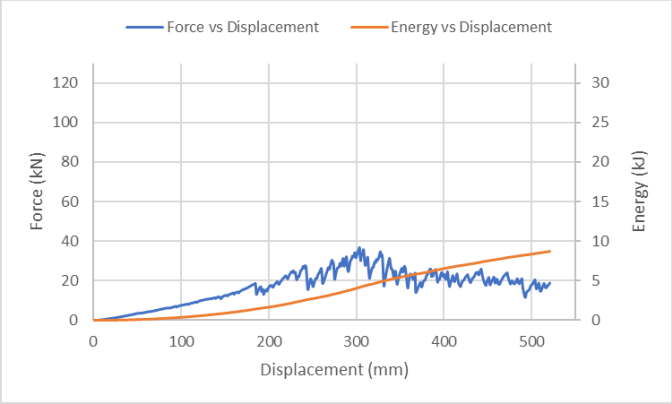

Fig. 6. Welded wire mesh (10.1-cm) representative testing results, force and energy versus displacement.

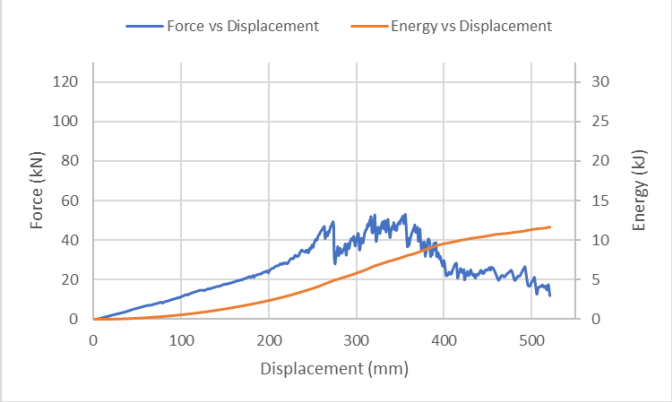

Fig. 7. Welded wire mesh (7.6-cm) representative testing results, force and energy versus displacement.

The first of the two synthetic meshes considered in this study consists of an engineered combination of synthetic netting substructure made of polyester and polyvinyl chloride (PVC) held to a synthetic webbing superstructure made of polyester straps (Figure 8). The sub-netting is sheathed in a synthetic material that provides extra protection to the fibres making up the sub-netting. This is tied to the polyester straps by steel C-rings. For the remainder of this paper, this mesh will be referred to as "polyester/PVC". As can be seen in Figure 8, the mesh itself is pinned down by bolting the large polyester straps, and the smaller polyester/PVC strands serve primarily to contain material that may fall through the larger straps.

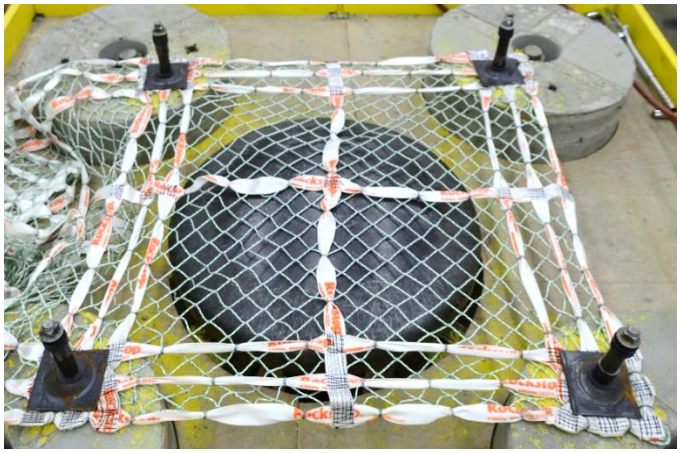

Fig. 8. Polyester/PVC mesh sample in place for HEHD testing.

The polyester/PVC mesh was tested under the same conditions as the chain-link and welded wire meshes previously discussed, and the performance characteristics of the synthetic mesh were then compared to the steel meshes. One of the tested polyester/PVC samples is shown at maximum displacement in Figure 9, and representative force-displacement and calculated energy-displacement curves from a total of three tests are shown in Figure 10. The average maximum load for the polyester/PVC samples was 99.3 kN (22.3 kips), occurring at an average ram displacement of 427 mm (16.8 in) and average calculated energy of 16.6 kJ (12,244 ft·lbf). These meshes maintained higher post-maximum strengths than all three steel mesh options, and the samples remained at least partially pinned to the reaction columns at all four points, with the sub-netting largely still intact. Overall, the calculated cumulative energy absorption of the meshes was 21.5 kJ (15,858 ft·lbf) at 500-mm (19.7 in) ram displacement, and the peak load value of 99.3 kN (22.3 kips) exceeded those of the chain-link, 7.6-cm (3-in), and 10.1-cm (4-in) welded meshes by 29.1, 46.1, and 62.7 kN (6.5, 10.4, and 14.1 kips), respectively.

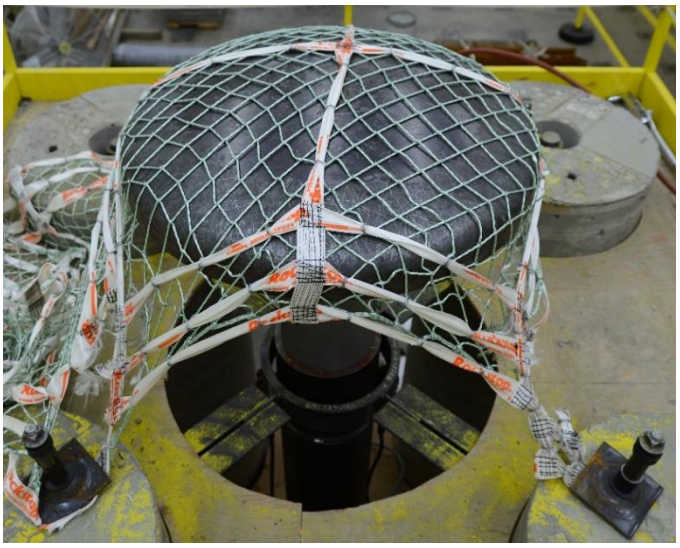

Fig. 9. Post-test photo of a polyester/PVC test sample, maximum ram displacement.

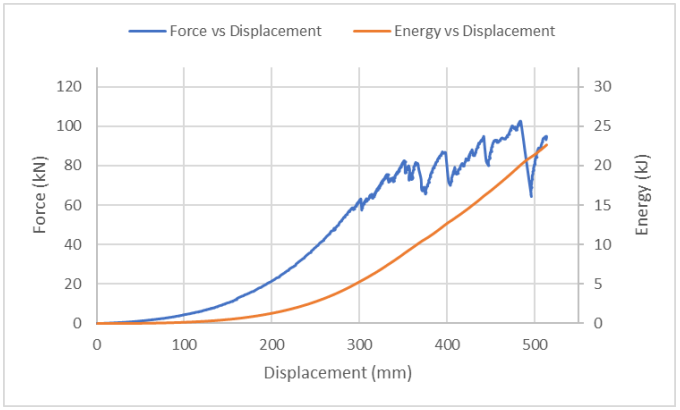

Fig. 10. Polyester/PVC mesh representative results, force and energy versus displacement.

A second type of synthetic mesh tested for this study is constructed in a grid-like structure similar to that of welded wire mesh, but is composed of tension-weaved high-strength polyethylene terephthalate (PET). Unlike the previous synthetic mesh sample, this mesh, referred to hereafter as “PET”, consists of one structure that serves both to contain small rocks and restrain larger rock mass movements. The grid-like structure is composed of individual bundles with 200x200-kN (45x45-kips) minimum tensile strength and 30-mm (1.2-in) apertures. This simple structure also means that the mesh can be pinned at any point as opposed to being restricted to certain axes along the product.

An additional product that may accompany the PET mesh is a thick, circular plastic plate to be used in place of conventional square steel plates. The plastic plates, shown in use with a PET sample in Figure 11, significantly reduce mesh shearing at pinned locations during material loading. The performance improvements are clearly demonstrated by the data.

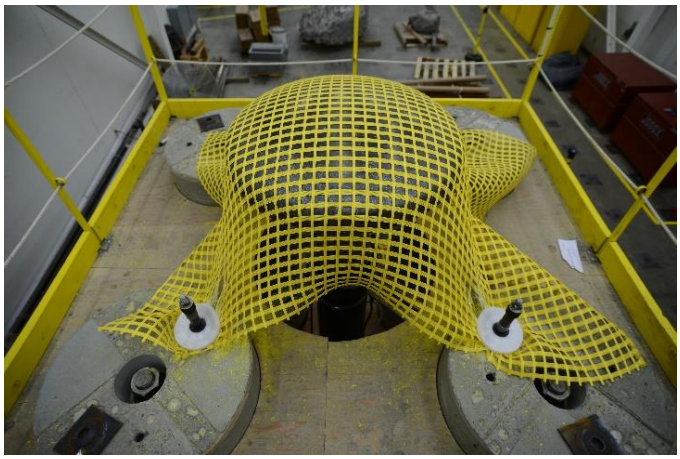

Fig. 11. PET mesh sample after HEHD testing, with circular plastic plates being used in place of conventional square steel plates.

Representative force-displacement and calculated energy-displacement curves from a total of three PET sample tests using conventional steel plates are shown in Figure 12, followed by the same curves from samples using plastic plates in Figure 13. When used with steel plates, mesh shear prevented the PET mesh from performing at levels similar to any of the three tested steel mesh types. The average maximum load for the PET/steel plate samples was 28.2 kN (6.3 kips), occurring at an average ram displacement of 296 mm (11.7 in) and average calculated energy of 3.9 kJ (2,876 ft·lbf). Using plastic plates, however, these values increased to 63.2 kN (14.2 kips) max force at 599 mm (23.6 in) displacement and 12.2 kJ (8,998 ft·lbf) absorbed energy. It is particularly important to note that the total ram stroke was 600 mm (23.6 in), meaning the mesh could possibly have continued taking load had the test been able to proceed. When instead used with the optional plastic plates in place of steel plates, the PET mesh was shown to be more effective than all three steel meshes in terms of energy absorbed before reaching peak load capacity and withstood roughly 30% greater displacement before reaching peak load only 10% less than the best performing steel mesh.

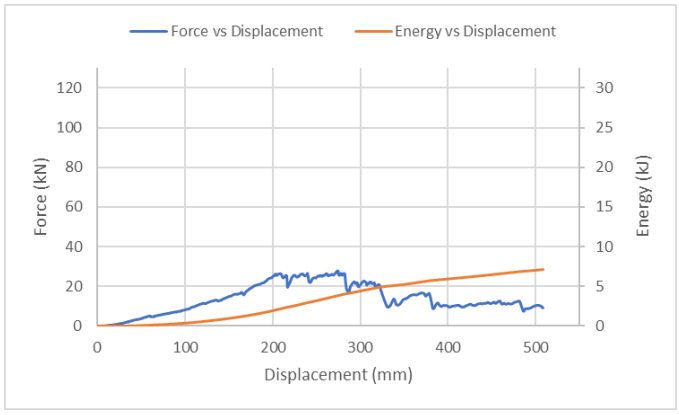

Fig. 12. PET mesh representative test results, force and energy versus displacement.

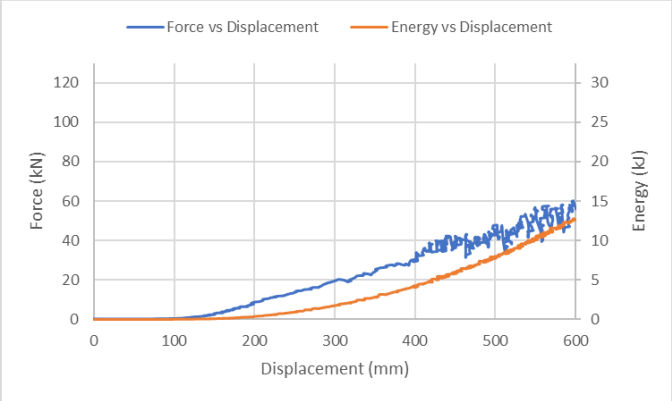

Fig. 13. PET mesh representative test results, force and energy versus displacement, with circular plastic plates instead of square steel plates.

4. DISCUSSION

To better understand the relative performance of the three types of steel mesh in comparison with the Polyester/PVC synthetic mesh, Figures 14 and 15 isolate the load-displacement and cumulative energy-displacement characteristics of each. To reiterate, these graphs show the comparison between the average performance characteristics of each steel mesh type and the individual performances of each of the three synthetic meshes presented above.

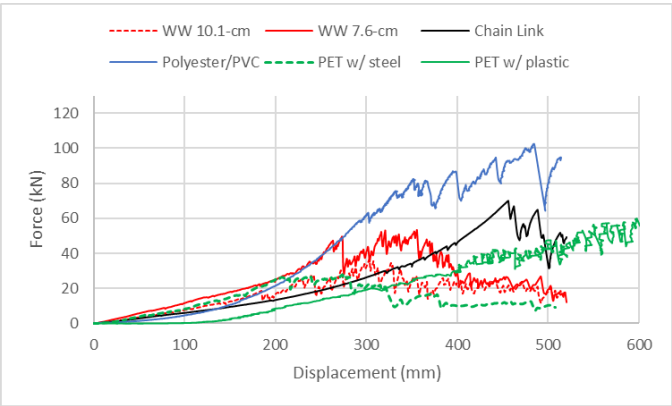

Fig. 14. Force-displacement curves for all types of mesh tested.

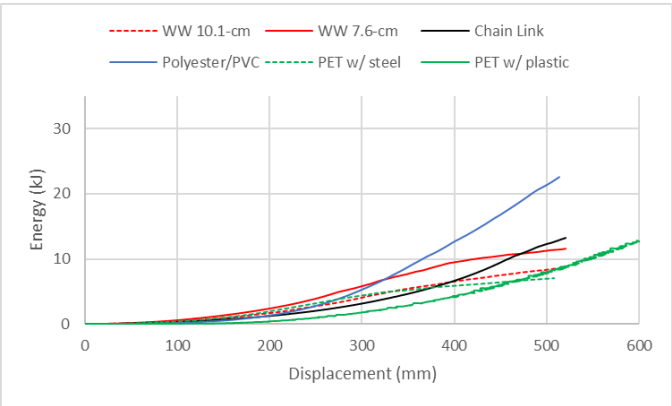

Fig. 15. Cumulative energy-displacement curves for all types of mesh tested.

Among the steel mesh options, both types of welded wire mesh were inferior to chain-link mesh in terms of peak load and energy absorption capacity. The chain-link mesh performed significantly better than the welded wire meshes in terms of peak load capacity, but at a cost in stiffness, as reflected in its much more modest energy absorption capacity relative to the welded wire meshes. The PET/steel plate combination was the weakest performer in all respects, but did provide a more rigid response to load than did the chain-link mesh. The polyester/PVC mesh outperformed all other meshes in every category, except for sustained load-bearing capacity where it, like all meshes aside from the PET/plastic plate combination, failed shortly after the 500-mm (19.7-in) mark. This indicates that in severe squeezing ground conditions where non-rigid ground support response can be tolerated, the PET/plastic plate combination may be an optimal choice. In terms of total energy absorption, the polyester/PVC mesh was the clear standout with a capacity nearly double the next closest mesh. This essentially means that per unit area, the Polyester/PVC mesh has the capability to provide more support capacity than the most commonly used steel mesh options for areal support in underground mining.

To address an issue raised in the introduction to this paper, an attempt has been made to index certain performance characteristics of the meshes included in this study. Table 1 provides the absolute values for peak load, energy absorption at peak load, maximum sample displacement at peak load, and energy absorption at 500 mm (19.7 in) of sample displacement. Table 2 relativizes these same values to the chain-link mesh performance results. Values greater than 100 indicate performance superior to chain-link mesh, while values less than 100 indicate poorer performance, in terms of percentage.

Table 1. Performance characteristics absolute values – peak load, energy at peak load, displacement at peak load, and energy at 500 mm displacement

Test Sample	Peak Load (kN)	Energy, Peak Load (kJ)	Displacement, Peak Load (mm)	Energy, 500 mm Displacement (kJ)
Chain-link	70.2	9.9	456	12.3
Welded wire (10.1-cm)	36.6	4.2	303	8.4
Welded wire (7.6-cm)	53.2	8.0	355	11.4

Polyester /PVC	99.3	16.6	427	21.5
PET	28.2	3.9	296	7.5
PET w/ plastic plates	63.2	12.2	599	7.5

Table 2. Performance characteristics relative values – peak load, energy at peak load, displacement at peak load, and energy at 500 mm displacement

Test Sample	Peak Load (kN)	Energy, Peak Load (kJ)	Displacement, Peak Load (mm)	Energy, 500 mm Displacement (kJ)
Chain-link	100	100	100	100
Welded wire (10.1-cm)	52	42	66	68
Welded wire (7.6-cm)	76	81	78	93
Polyester /PVC	142	168	94	175
PET	40	39	65	61
PET w/ plastic plates	90	123	131	61

To close out this discussion, there are additional performance factors to consider regarding each of the mesh types included in this paper. These considerations may not have direct impact on mesh performance as it relates to load and energy absorption capacity, but they provide guidance regarding specific use. In other words, all three mesh types may be used in a single mine depending on the specific scenario:

- Corrosion – steel meshes are prone to corrosion when used in corrosive environments and mitigating strategies such a galvanized or stainless steels are generally more costly than periodic rehabilitation. Both synthetic meshes discussed in this paper are resistant to corrosion, the one exception being the C-rings used in the polyester/PVC mesh. Corrosion of these rings could lead to separation of the sub-netting from the belt superstructure, the consequence of which being a loss of small rock containment. Additionally, though outside the scope of this study, laboratory and field observations have shown the PET mesh to be effective in environments with pH levels up to 9, indicating its resistance to acidic corrosion. Consequently, the PET mesh along with optional plastic plates would be the most corrosion-resistant option discussed in this paper.
- Flammability – both synthetic meshes have undergone flammability testing for safe use in mines, and the PET mesh specifically has passed US Mine Safety and Health Administration (MSHA) flame retardant testing. Steel meshes however are inflammable, and though their strength properties may be reduced by excessive heat exposure, steel meshes are less likely than synthetic meshes to be damaged by mine fires.
- Blast and impact damage – all mesh types are susceptible to blast damage, but the potential for loss of rock containment in active headings using blasting is greater for synthetic meshes. Similarly, damage resulting from vehicle impact may be greater for synthetic meshes due to their lack of rigidity. An offsetting factor in this case would be that frayed steel meshes produce jagged material that may snag and cut miners, whereas frayed synthetic meshes would not produce similar hazards.
- Handling – the rigidity of welded-wire meshes makes their alignment and placement significantly easier than spooled materials, and steel meshes' resistance to tearing makes it significantly easier to stretch and pack during placement. Conversely, synthetic meshes are drastically lighter per unit area than steel meshes, easing transport and placement without machine aid, and the PET mesh has no metal parts that may snag or cut handlers.

5. CONCLUSION

The SMRD-developed HEHD testing machine was used to perform quasi-static tests on conventional steel meshes and new synthetic mesh alternatives. The intent was to better understand the mechanics of yielding mesh support systems for use in weak-rock or high-stress mining environments where either squeezing or rockburst-prone ground is present. This work provides insight into the behaviour of surface support and a number of conclusions can be drawn from these initial test series.

The (1) peak load, (2) energy absorption at peak load, (3) maximum sample displacement at peak load, and (4) energy absorption at 500 mm (19.7 in) displacement constituted the performance characteristics used to assess (1) 5-cm (2-in) aperture chain-link, (2) 7.5-cm (3-in) aperture welded wire, (3) 10-cm (4-in) aperture welded wire, (4) a polyester/PVC mesh option, and (5) a PET mesh option. Using these performance characteristics, an index was introduced to begin the process of standardizing areal mesh support comparison. It is hoped that this will benefit both the scientific understanding of underground mining mesh support systems, as well as

provide industry a quick-reference tool for determining appropriate products for effective ground support plans.

Currently, these mesh samples have been tested only under quasi-static loading conditions. In the future, this information will need to be supplemented by data from fully dynamic tests. These tests will need to subject mesh support systems to very high displacement rates to allow these various surface support types to be evaluated under true dynamic conditions. Additional quasi-static tests assessing additional steel and synthetic meshes will also be needed to mature the mesh support system index started by the current study. This study was only a first step, but an important one to build upon as part of the SMRD mission of improving the health and safety of underground metal mine workers.

6. ACKNOWLEDGEMENT

The authors thank Seth Finley, Steve Murray, Adrian Berghorst, Mel Briers, and Paul Janson for their assistance with mesh preparation and testing, and Carl Sunderman and Greg Feagan for setting up the electronics and instrumentation for data collection. The authors would also like to thank Lewis Martin, Curtis Clark, and Mike Stepan for their helping during their time at SMRD.

The findings and conclusions in this paper have not been formally disseminated by NIOSH and should not be construed to represent any agency determination or policy. Mention of any company or product does not constitute endorsement by NIOSH.

REFERENCES

1. Hadjigeorgiou, J. and Stacey, T.R. (2018). Challenges in determining the capacity of mesh. In *AusRock 2018: The 4th Australasian Ground Control in Mining Conference*, Australasian Institute of Mining and Metallurgy, Carlton, pp. 280-290.
2. Kaiser, P.K., Tannant, D.D., and McCreath, D.R. (1996). *Canadian Rockburst Support Handbook*, Geomechanics Research Centre, Laurentian University, Sudbury.
3. Kalenchuk, K., Palleske, C., Hume, C., and Oke, J. (2020). Support design and implementation in difficult ground conditions – managing the expected and unexpected. In C.C. Li, H. Odegaard, A.H. Hoien, and J. Macias (eds), *Proceedings of Eurock 2020 – Hard Rock Engineering*, Trondheim, Norway.
4. Kirsten, H.A.D. and Labrum, P.R. (1990). The equivalence of fibre and mesh reinforcement in the shotcrete used in tunnel-support systems. *Journal of the South African Institute of Mining and Metallurgy*, vol. 90, pp. 153-171.
5. Martin, L., Clark, C., Johnson, J., and Stepan, M. (2015). A new high force and displacement shotcrete test. Paper presented at the 2015 SME Annual Conference & Expo, Denver, 15-18 February.
6. Morton, E.C., Thompson, A.G., and Villaescusa, E. (2007). Testing and analysis of steel wire mesh for mining applications of rock surface support. In L Sousa, C Olalla & N Grossmann (eds), *Proceedings of the 11th Congress of the International Society for Rock Mechanics, International Society for Rock Mechanics*, Lisbon, pp. 1061-1064.
7. Ortlepp, W.D. (1969). An empirical determination of the effectiveness of rockbolt support under impulse loading. In T Bekke & F Jorstad (eds), *Proceedings of the International Symposium on Large Permanent Underground Openings*, Oslo, pp. 197-205.
8. Ortlepp, W.D. (1983). Considerations in the design of support for deep hard-rock tunnels. In *Proceedings of the 5th International Congress of the International Society for Rock Mechanics*, Australian Geomechanics Society, Melbourne, pp. D179-187.
9. Ortlepp, W.D. and Stacey, T.D. (1998). Performance of tunnel support under large deformation static and dynamic loading. *Tunneling and Underground Space Technology*, Vol. 13, pp. 15-21.
10. Pakalnis, V. and Ames, D. (1983). Load tests on mine screening. In *Underground Support Systems*, Canadian Institute of Mining, Metallurgy and Petroleum, Westmount.
11. Player, J.R., Morton E.C., and Villaescusa, E. (2008). Static and dynamic testing of steel wire mesh for mining applications of rock surface support. In *Proceedings of the 6th International Symposium on Ground Support in Mining and Civil Engineering Construction*, Cape Town, pp. 693-706.
12. Potvin, Y., Wesseloo, J., and Heal, D. (2010). An interpretation of ground support capacity submitted to dynamic loading. In M. Van Sint Jan & Y Potvin (eds), *Proceedings of the 5th International Seminar on Deep and High Stress Mining*, Santiago, pp. 251-272.
13. Potvin, Y. and Hadjigeorgiou, J. (2020). Ground Support in Underground Mines. Australian Centre for Geomechanics, Crawley, Western Australia.
14. Roberts, M.K.C. and Brummer, R.K. (1988). Support requirements for rockburst conditions. *Journal of South African Institute of Mining and Metallurgy*, Vol. 88, pp. 97-104.
15. Stacey, T.R., Ortlepp, W.D., and Kirsten, H.A.D. (1995). Energy-absorption capacity of reinforced shotcrete, with reference to the containment of rockburst damage. *Journal of the South African Institute of Mining and Metallurgy*, Vol. 95, pp. 137-140.
16. Tannant, D. and Kaiser, P.K. (1997). Evaluation of shotcrete and mesh behaviour under large imposed deformations. In *Proceedings of the International Symposium on Rock Support*, Lillehammer, pp. 782-792.
17. Wagner, H. (1984). Support requirements for rockburst conditions. In *Proceedings of the 1st International Congress on Rockbursts and Seismicity in Mines*, Johannesburg, pp. 209-218.